Wideband Dual-polarized Vivaldi Antenna with Gain Enhancement

Huanhuan Lv, Qiulin Huang *, Jianqiang Hou, and Jinlin Liu

National Laboratory of Science and Technology on Antennas and Microwaves
Xidian University, Xi'an, 710071, China
lvhuanhuan4213@126.com, *qiulhuang@mail.xidian.edu.cn, houjq@163.com, xdjinlinliu@126.com

Abstract ─ A wideband dual-polarized Vivaldi antenna covering 1.85-18.3 GHz band with enhanced gain is presented in this letter. The proposed antenna consists of two Vivaldi antenna elements (VAEs), which are designed based on the conventional Vivaldi antenna. Dual-slot structure is employed to improve the gain of the conventional Vivaldi antenna. As a result, spherical-like waves across the slot aperture of the conventional Vivaldi antenna can be transformed to be plane-like waves and thus gain enhancement can be achieved. In order to extend lower frequency limit of the VAE, elliptical slots are adopted. The proposed dual-polarized Vivaldi antenna is obtained by combining two VAEs in a cross-shaped form. The prototype is simulated, fabricated, and measured. A good agreement between EM simulated and measured results evidently validates the proposed antenna.

Index Terms ─ Dual-polarized Vivaldi antenna, enhanced radiation characteristics, wideband.

I. INTRODUCTION

Vivaldi antenna has been widely used in the wideband communication system owing to the features of planar structure, low profile, ease of fabrication and compatibility with backend circuits since its appearance in 1979 [1]. Moreover, modern antenna measurement systems such as material testing systems or near-field antenna measurement systems require antennas with the capability of dual-polarization. In recent years, dual-polarized Vivaldi antenna has attracted considerable interests.

A common way to design dual-polarized Vivaldi antennas is to place two Vivaldi antenna elements (VAEs) orthogonally along the edge. Wideband dual-polarized antenna arrays based on this placement method are presented in [2-5]. However, for single dual-polarized antenna, this placement method causes displacement of the phase center between two VAEs. In [6], a dual-polarized cross-shaped Vivaldi antenna covering 0.7 to 7.3 GHz is presented, which obtains good cross-polarization isolation.

One of the challenges in designing the Vivaldi antenna is to improve the gain. In [7-10], corrugated ripples are used to reduce the current distribution along the antenna edge to achieve gain enhancement. In [11], a dual-polarized cross-shaped Vivaldi embedded in a dielectric is presented, which obtains a maximum gain value of 10.5 dBi.

In this letter, a wideband dual-polarized Vivaldi antenna covering 1.85-18.3 GHz band for the antenna measurement system is presented. Two VAEs are placed in a cross-shaped form to achieve dual-polarization. The VAE is modified from the conventional Vivaldi antenna by introducing dual-slot structure, which can improve the gain without increasing size of the antenna. Elliptical slots are adopted to extend lower frequency limit of the Vivaldi antenna and the radiation characteristics at lower frequencies are improved. The proposed dual-polarized Vivaldi antenna is simulated, fabricated, and measured. The measured results show that the proposed antenna features wideband, high gain and good cross-polarization isolation performance.

II. ANTENNA DESIGN

Figure 1 illustrates evolution process of the VAE. Three antennas denoted as Ant I, Ant II and Ant III are designed on the Rogers RO4350 substrate with relative permittivity ε_r = 3.66. The radiation surfaces are printed on the top side of the substrate and feedlines are printed on the other side of the substrate. Three antennas have the same size of 145 mm × 58 mm × 0.5 mm. Simulated S_{11} and boresight (Phi = 0°, Theta = 90°) gain of Ant I, Ant II and Ant III are shown in Fig. 2. The simulated results are obtained by using High Frequency Structure Simulation (HFSS) software with Finite Element Method (FEM).

Ant I is a conventional Vivaldi antenna, whose lower frequency is set as 2.6 GHz. It is known that lower frequency of a Vivaldi antenna is related to the aperture width, which is denoted as W_1 in Fig. 1. The reason for setting an initial frequency higher than the required lower frequency (1.85 GHz) is to maintain a relatively compact size before the optimization. The aperture width

Submitted On: December 4, 2017
Accepted On: September 9, 2018

W_1 is set to be 58 mm based on analysis in [12]. Tapered transmission lines are used to feed the antenna to improve impedance matching. Exponential curves y_{c1} and y_{c2} of Ant I are described by the equations as follows:

$$y_{c1} = 0.00001254e^{0.13x} + 0.6 \qquad 0 \le x \le L_2, \tag{1}$$

$$y_{c2} = -0.00001254e^{0.13x} - 0.6 \qquad 0 \le x \le L_2. \tag{2}$$

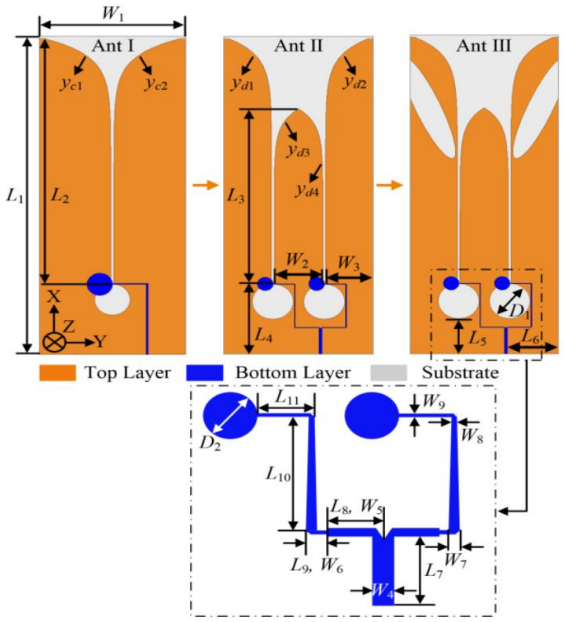

Fig. 1. Evolution process of VAE.

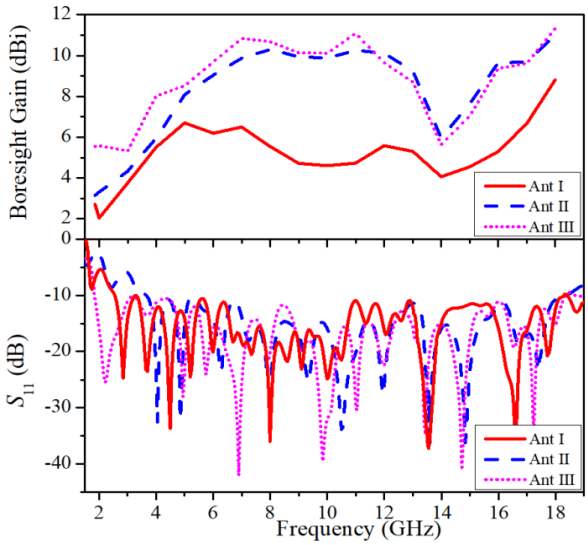

Fig. 2. Simulated S_{11} and boresight (Phi = 0°, Theta = 90°) gain of Ant I, Ant II and Ant III.

It can be seen from Fig. 2 that -10 dB impedance bandwidth of Ant I can cover 2.6-18.3 GHz band with maximum boresight gain of 6.7 dBi. To improve boresight gain without introducing a dimensional increase, dual-slot structure is used to design Ant II as shown in Fig. 1. Four exponential curves denoted as y_{d1}, y_{d2}, y_{d3} and y_{d4} can be described by the equations as follows:

$$y_{d1} = 0.000007837e^{0.13x} + 10.5 \qquad 0 \le x \le L_2, \tag{3}$$

$$y_{d2} = -0.000007837e^{0.13x} - 10.5 \qquad 0 \le x \le L_2, \tag{4}$$

$$y_{d3} = -0.00004324e^{0.15x} + 9.5 \qquad 0 \le x \le L_3, \tag{5}$$

$$y_{d4} = 0.00004324e^{0.15x} - 9.5 \qquad 0 \le x \le L_3. \tag{6}$$

Accordingly, the feedline is changed to a T-shaped network. In contrast to traditional Vivaldi antenna, dual-slot structure can generate two columns of in-phase waves with equal amplitudes, which are mutually coupled across the aperture.

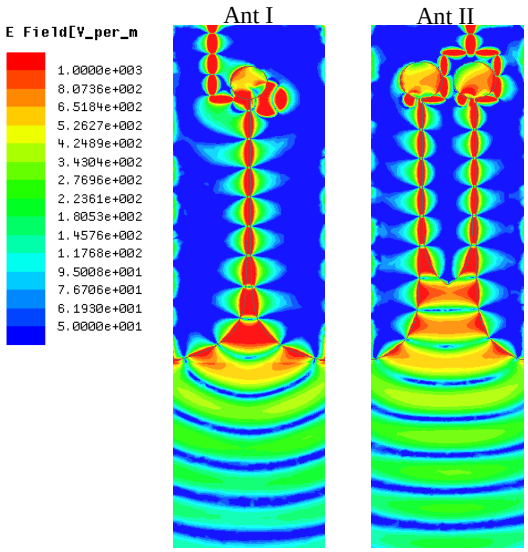

Fig. 3. Simulated electric field distributions of Ant I and Ant II at 10 GHz.

Shown in Fig. 3 are simulated electric field distributions of Ant I and Ant II at 10 GHz. It can be observed that compared with spherical-like waves across the slot aperture of Ant I, waves generated by dual-slot structure are plane-like waves, which can produce high boresight gain. However, the aperture size of each slot in Ant II is actually reduced compared with Ant I and the lower frequency of VAE is increased as shown in Fig. 2. In order to solve this problem to meet the required lower frequency, elliptical slots are etched in Ant III as shown in Fig. 1. Simulated surface current flow of Ant II and Ant III at 1.85 GHz is shown in Fig. 4 to illustrate the operating characteristics of the elliptical slots at lower frequencies. It can be seen that the effective length of the surface current path is visibly lengthened with the utilization of elliptical slots and new resonant mode can be introduced to enhance the radiation characteristics at lower frequencies. It can be observed from Fig. 2 that -10 dB impedance bandwidth of Ant III can cover 1.85 GHz to 18.3 GHz. Thus, Ant III is chosen as the final VAE.

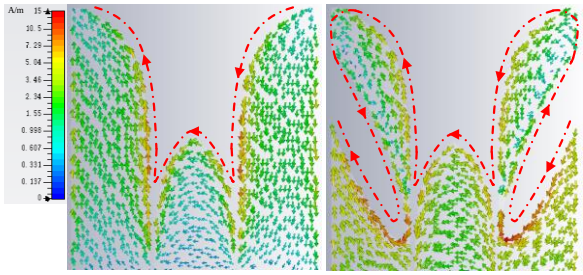

Fig. 4. Simulated surface current flow of Ant II and Ant III at 1.85 GHz.

III. SIMULATION AND TEST OF ANTENNA

HFSS with FEM is used to simulate and optimize the proposed VAE. The numerical analysis procedure is demonstrated as follows. In this paper the parameters under study include the total length of radiation slot line L_2, the length of middle structure L_3 and the location of elliptical slot L_e. The results are obtained when one single parameter is changed and other parameters are constant.

A. The influence of L_2 on the performance of VAE

The effect of varying the total length of radiation slot line L_2 on S_{11} of VAE is shown in Fig. 5. It can be seen that with increasing L_2 from 112 mm to 132 mm, S_{11} curves in low frequency bands have larger changes and stop-bands occur around 2.6 GHz. And with decreasing L_2 from 112 mm to 102 mm, S_{11} curves also cannot fully cover 1.85-18.3 GHz. Therefore, the optimal value L_2 = 112 mm is obtained.

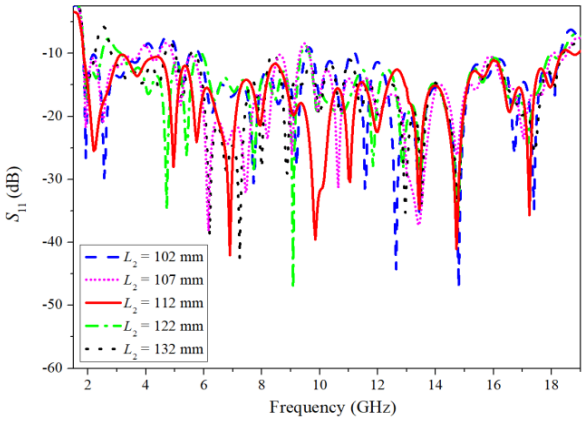

Fig. 5. Simulated S_{11} of VAE under different values of L_2.

B. The influence of L3 on the performance of VAE

The initial value of length L_3 is set based on the design rule:

$$L_3 > \max\{0.5\lambda_{max}, 2\lambda_{min}\}, \quad (7)$$

where λ_{min} and λ_{max} stand for the minimum and maximum wavelengths in the operation band [13]. The length L_3 has direct influence on the coupling effect between waves generated by dual-slot structure. Thus the length L_3 has significant effect on the bandwidth of VAE. Figure 6 shows simulated S_{11} of VAE under different values of L_3. It can be seen that when L_3 is equal to 62 mm or 72 mm, lower frequency of VAE cannot cover 1.85 GHz. And a stop-band occurs around 4 GHz when L_3 is increased. Hence, the length L_3 is set to be 82 mm.

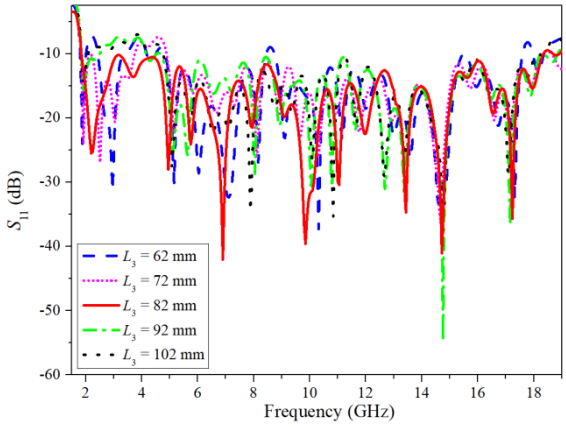

Fig. 6. Simulated S_{11} of VAE under different values of L_3.

C. The influence of L_e on the performance of VAE

The major axis and minor axis of the elliptical slot are 25 mm and 5 mm. This paper is focused on the location of elliptical slot, which has direct influence on the surface current distribution. Figure 7 shows simulated S_{11} of VAE under different values of L_e. As depicted in Fig. 7, a stop-band is presented around 3 GHz when L_e is equal to 52 mm or 47 mm, and as L_e arrives at 62 mm and 57 mm, two stop-bands are presented around 5 GHz and 9 GHz. To obtain good performance from 1.85 GHz to 18.3 GHz, the position of elliptical slot L_e is optimized to be 57 mm.

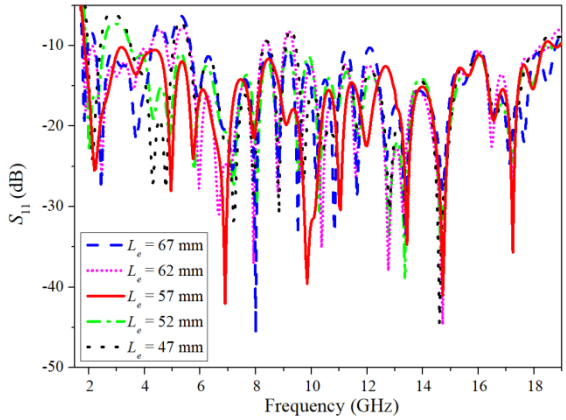

Fig. 7. Simulated S_{11} of VAE under different values of L_e.

D. Configuration of dual-polarized Vivaldi antenna

By combining two VAEs in a cross-shaped form, the proposed dual-polarized Vivaldi antenna is obtained. Figure 8 (a) shows the implementation details of proposed dual-polarized Vivaldi antenna. Two complementary cuboid slots are cut in substrates of VAEs for mounting the VAEs orthogonally. The lengths of two cuboid slots are 133.9 mm and 11.1 mm and the widths of two cuboid slots are 0.5 mm.

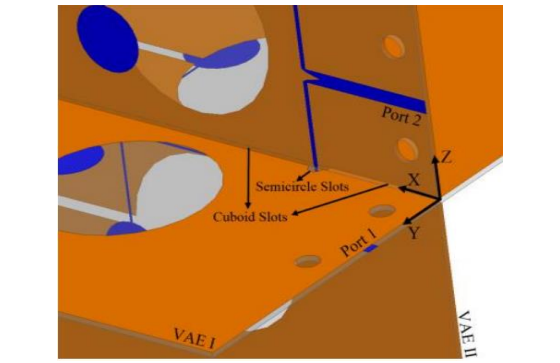

(a)

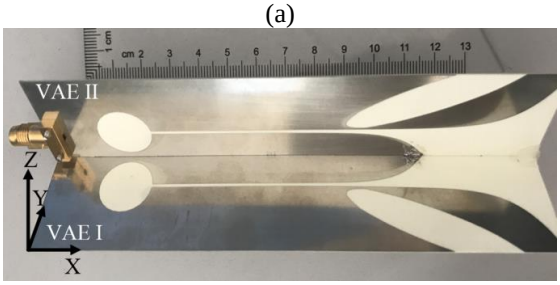

(b)

Fig. 8. (a) Implementation details and (b) photograph of the proposed cross-shaped dual-polarized Vivaldi antenna.

In order to avoid feedlines overlapping, feedlines of two VAEs are staggered to each other and that means line L_7 is shortened while L_{10} is lengthened to keep the total length of feedline unchanged. Thus, the phase center of VAE can remain the same. The stagger distance between two feedlines is optimized to be 2 mm. As shown in Fig. 8 (a), two semicircle slots are etched in radiation surfaces of VAEs to avoid galvanic contact between feedlines and radiation surfaces. Besides, mounting holes are cut in substrates for RF connectors. The optimized dimensions of the VAE are given as follows (all in mm): L_1 = 145, L_2 = 112, L_3 = 82, L_4 = 32, L_5 = 16, L_6 = 19.91, L_7 = 12, L_8 = 8.3, L_9 = 1.86, L_{10} = 19.72, L_{11} = 8.58, L_e = 57, W_1 = 58, W_2 = 19, W_3 = 18.5, W_4 = 1.18, W_5 = 0.36, W_6 = 0.2, W_7 = 0.32, W_8 = 0.16, W_9 = 0.2, D_1 = 16, D_2 = 6.1. A prototype of the proposed dual-polarized Vivaldi antenna is fabricated as shown in Fig. 8 (b).

E. Test of antenna

Simulated and measured *S*-parameters are shown in Fig. 9. The measurement is performed on an Agilent 8720ES network analyzer. It can be seen that the proposed dual-polarized Vivaldi antenna can cover 1.85-18.3 GHz band with S_{11} better than -10 dB. The measured isolation level between two VAEs across operation band is better than -25 dB. The discrepancies between simulated and measured results may be caused by fabrication errors, the variation of material properties and extra loss of the RF connectors.

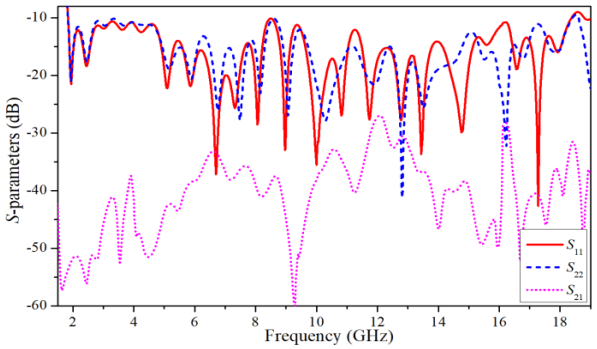

(a)

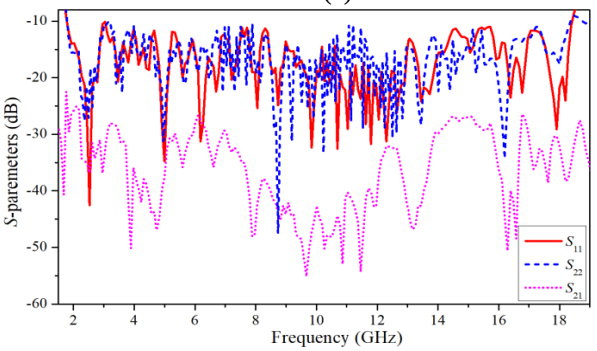

(b)

Fig. 9. (a) Simulated and (b) measured *S*-parameters of the proposed antenna.

Figure 10 presents measured normalized radiation patterns of the proposed antenna prototype at 1.85 GHz, 6 GHz, 13 GHz and 18 GHz. The patterns are presented in xoy and xoz planes with the same coordinate system shown in Fig. 8 and each plane contains both polarization components (co-polarization and cross-polarization). The results are obtained when one VAE is excited and the other one is terminated to a 50Ω load. It can be seen that radiation patterns of VAE I in xoy plane are similar to radiation patterns of VAE II in xoz plane due to the orthogonal orientation of two VAEs.

Figure 11 presents simulated and measured boresight gain of the proposed antenna. The results are obtained when one VAE is excited and the other one is terminated to a 50Ω load. It can be seen that gain values at lower frequencies are higher than 4 dBi and peak gain values of VAE I and VAE II are as high as 11.3 dBi and 11.18 dBi. Figure 12 presents measured cross-polarization isolation as a function of frequency in the boresight direction. It can

be seen that cross-polarization isolation of the proposed antenna is better than 16.5 dB across 1.85-18.3 GHz band, which means that the power ratio of radiated cross-polarized components to the co-polarized components is less than 2.2%. Table 1 shows comparisons between this work and previous research. The proposed antenna obtains good gain performance with compact aperture width in the operation band.

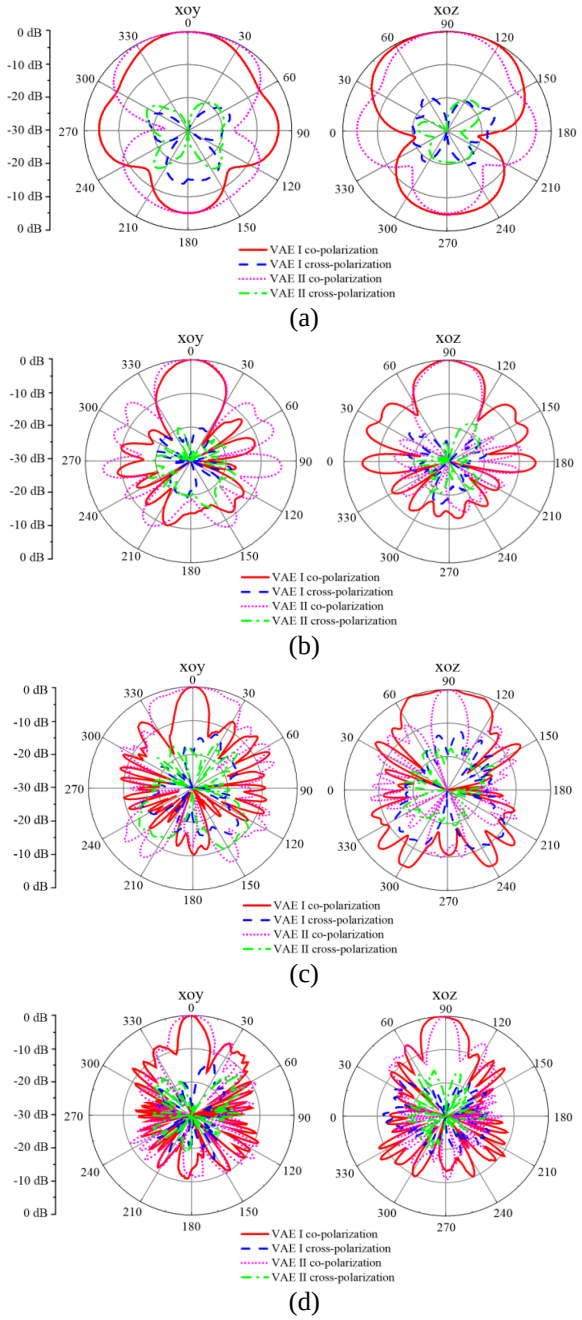

Fig. 10. Measured normalized radiation patterns of the proposed antenna in xoy and xoz planes at: (a) 1.85 GHz, (b) 6 GHz, (c) 13 GHz, and (d) 18 GHz.

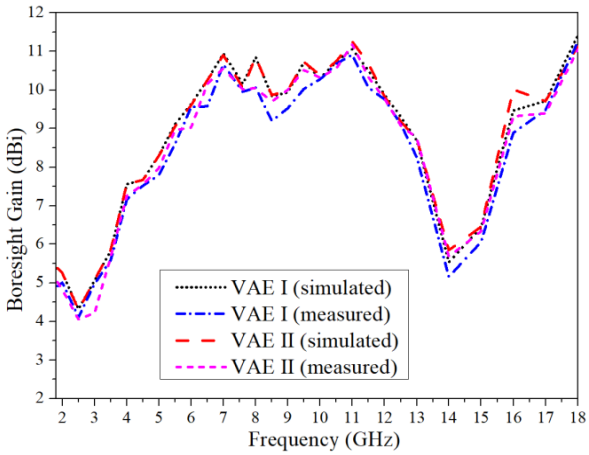

Fig. 11. Simulated and measured boresight gain of the proposed antenna.

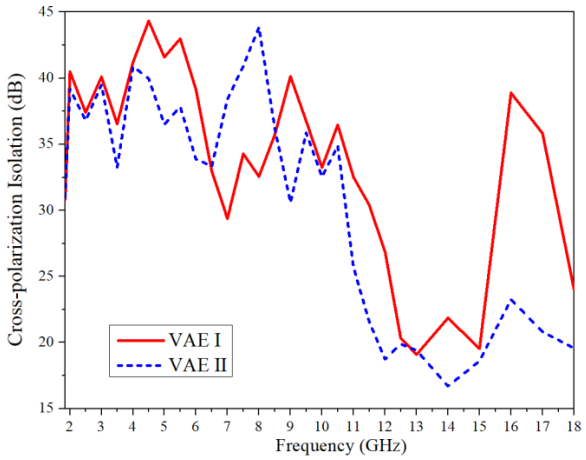

Fig. 12. Measured cross-polarization isolation in the boresight direction of the proposed antenna.

Table 1: Comparisons between this work and previous research

Ref.	Fractional Bandwidth (GHz)	Aperture Width (mm)	Aperture Width/ λ_{max}	Gain (dBi)
6	0.7-7.3	220	0.51	3.8-11.2
8	1.4-12	110	0.51	4-11.3
9	0.8-3.8	150	0.4	2.4-8.1
This work	1.85-18.3	58	0.36	4.06-11.3

Note: λ_{max} stands for maximum wavelength in the operation band.

IV. CONCLUSION

A wideband dual-polarized Vivaldi antenna covering 1.85-18.3 GHz band is presented in this letter. The proposed antenna consists of two VAEs, which are placed in a cross-shaped form to achieve dual-polarization.

Dual-slot structure is utilized and optimized to enhance radiation characteristics. Elliptical slots are used to extend lower frequency limit and enhance the radiation characteristics at lower frequencies. A prototype of the proposed dual-polarized Vivaldi antenna is fabricated and measured. Measured results agree well with simulated ones and the proposed antenna is qualified to be used in modern antenna measurement systems.

REFERENCES

[1] P. J. Gibson, "The Vivaldi aerial," *1979 9th European Microwave Conference*, pp. 101-105, 1979.

[2] J. Remez, A. Segal, and R. Shansi, "Dual-polarized wide-band wide scan multi-beam antenna system from tapered slot-line elements array," *IEEE Antennas and Wireless Propagation Letters*, vol. 4, pp. 293-296, 2005.

[3] M. Elsallal and J. Mather, "An ultra-thin, decade (10:1) bandwidth, modular "BAVA" array with low cross-polarization," *2011 IEEE International Symposium on Antennas and Propagation (APSU RSI)*, pp. 1980-1983, July 2011.

[4] R. W. Kindt and W. R. Pickles, "Ultrawideband all-metal flared-notch array radiator," *IEEE Transactions on Antennas and Propagation*, vol. 58, no. 11, pp. 3568-3575, Nov. 2010.

[5] J. B. Yan, S. Gogineni, B. Camps-Raga, and J. Brozena, "A dualpolarized 2–18-GHz Vivaldi array for airborne radar measurements of snow," *IEEE Transactions on Antennas and Propagation*, vol. 64, no. 2, pp. 781-785, Feb. 2016.

[6] M. Sonkki, D. Sanchez, V. Hovinen, E. T. Salonen, and M. Ferrando, "Wideband dual-polarized cross-shaped Vivaldi antenna," *IEEE Transactions on Antennas and Propagation*, vol. 63, no. 6, pp. 2813-2819, June 2015.

[7] F. B. Zarrabi, N. P. Gandji, R. Ahmadian, H. Kuhestani, and Z. Mansouri, "Modification of Vivaldi antenna for 2-18 GHz UWB application with substrate integration waveguide structure and comb slots", *Applied Computational Electromagnetics Society Journal*, vol. 30, no. 8, pp. 844-849, Aug. 2015.

[8] H. Xu, J. Lei, C. J. Cui, and L. Yang, "UWB dual-polarized Vivaldi antenna with high gain," *2012 International Conference on Microwave and Millimeter Wave Technology (ICMMT)*, pp. 1-4, May 2012.

[9] Y. Z. Zhu, D. Y. Su, W. X. Xie, Z. H. Liu, and K. W. Zuo, "Design of a novel miniaturized Vivaldi antenna with loading resistance for ultra wideband (UWB) applications," *Applied Computational Electromagnetics Society Journal*, vol. 32, no. 10, pp. 895-900, Oct. 2017.

[10] M. A. Ashraf, K. Jamil, A. R. Sebak, M. Shoaib, Z. Alhekail, M. Alkanhal, and S.Alshebeili, "Modified antipodal Vivaldi antenna with shaped Elliptical corrugation for 1-18 GHz UWB application," *Applied Computational Electromagnetics Society Journal*, vol. 30, no. 1, pp. 68-77, Jan. 2015.

[11] G. Adamiuk, T. Zwick, and W. Wiesbeck, "Compact, dual-polarized UWB-antenna, embedded in a dielectric," *IEEE Transactions on Antennas and Propagation*, vol. 58, no. 2, pp. 279-286, Feb. 2010.

[12] R. Janaswamy and D. H. Schaubert, "Characteristic impedance of a wide slotline on low-permittivity substrates (short paper)," *IEEE Transactions on Microwave Theory and Techniques*, vol. 34, no. 8, pp. 900-902, Aug. 1986.

[13] J. Lee, *Antenna Engineering Handbook*. 4th ed., New York: McGraw-Hill, 2007.

Huanhuan Lv received his B.S. and M.S. degrees from Xidian University, Xi'an, Shaanxi, China, in 2013 and 2016, respectively. He is currently working towards the Ph.D. degree in Electromagnetic Field and Microwave Technology at Xi'dian University, Xi'an, Shaanxi, China. His research interests are in wideband antennas, arrays and microwave circuits.

Qiulin Huang received his B.S. and Ph.D. degrees from Xidian University, Xi'an, Shaanxi, China, in 2001 and 2007, respectively. In 2002, he joined the School of Electronic Engineering at Xidian University. His research interests include smart antennas and arrays, and satellite navigation and anti-interference technology.

Jianqiang Hou received his B.S., M.S. and Ph.D. degrees from Xidian University, Xi'an, Shaanxi, China, in 1999, 2004 and 2010, respectively. In 2006, he joined the School of Electronic Engineering at Xidian University. His research interests include microwave circuit and system, antennas, and electromagnetic compatibility.

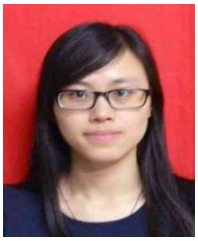

Jinlin Liu received her M.S. degree in Electromagnetic Field and Microwave Technology from Xidian University, Xi'an, Shaanxi, China, in 2016. She is currently working toward the Ph.D. degree in Electromagnetic Field and Microwave Technology at Xidian University. Her research interests include design of antennas, and microwave circuits.